



## Effects of *Alpinia oxyphylla* fructus polysaccharide on the gelatinization, retrogradation, structural characteristics, antioxidant activity, and in vitro digestibility of corn starch

Zihan Li<sup>a</sup>, Qingfei Duan<sup>b</sup>, Yongmei Mo<sup>a</sup>, Fuhan Xie<sup>a</sup>, Qian Zhou<sup>a</sup>, Pingping Sun<sup>a</sup>, Changfu Lu<sup>c</sup>, Fengwei Xie<sup>d,\*</sup>, Pei Chen<sup>a,\*</sup>

<sup>a</sup> Guangdong Provincial Key Laboratory of Food Quality and Safety, College of Food Science, South China Agricultural University, Guangzhou, Guangdong 510642, China

<sup>b</sup> Institute of Chemistry, Henan Academy of Sciences, Zhengzhou, 450002, China

<sup>c</sup> Yangjiang Baguosheng Food Co., Ltd., Guangdong, Yangjiang, 529500, China

<sup>d</sup> Department of Chemical Engineering, University of Bath, Bath BA2 7AY, United Kingdom

### ARTICLE INFO

#### Keywords:

*Alpinia oxyphylla* fructus polysaccharide  
Corn starch  
Properties

### ABSTRACT

*Alpinia oxyphylla* fructus polysaccharide (AOF) exhibits diverse biological activities, but its influence on starch properties remains underexplored. This study elucidates the effects of AOF on the gelatinization, retrogradation behavior, and functional characteristics of corn starch (CS). Iodine binding capacity, XRD, and FTIR analyses revealed that AOF significantly inhibited amylose leaching, likely through hydrogen bonding interactions, thereby suppressing starch recrystallization and retrogradation. At a 6 % AOF concentration, the relative crystallinity of the system decreased from  $14.910 \pm 0.320$  % to  $6.023 \pm 0.142$  % on Day 7, the retrogradation rate ( $R_7$ ) declined from  $54.95 \pm 1.07$  % to  $32.58 \pm 1.08$  %, and the gel hardness was reduced from  $187.32 \pm 1.87$  gf to  $66.06 \pm 1.08$  gf. Additionally, AOF significantly increased the resistant starch (RS) content from  $10.96 \pm 0.38$  % to  $19.08 \pm 1.06$  % and enhanced the antioxidant capacity of the composite system, with ABTS<sup>+</sup> and DPPH radical scavenging activities increasing by  $88.59 \pm 1.1526$  % and  $76.24 \pm 1.3277$  %, respectively. These findings collectively demonstrate that AOF is a functional ingredient capable of modulating both structural and functional properties of starch-based foods.

### 1. Introduction

*Alpinia oxyphylla* fructus (AOF), one of China's four principal southern medicinal herbs, is traditionally used to warm the spleen and kidneys, alleviate diarrhea, and is widely used in culinary and preserved fruit applications [1]. The town of Daba in Yangdong District, Yangjiang City, is the largest AOF cultivation and processing base in Guangdong Province, with about 12,000 mu of cultivation area and an annual yield of approximately 50 tons [2]. The majority of the production is utilized for medicinal purposes, while only a small portion is used for food processing, such as candied products. The bioactive components of AOF are complex, including essential oils, flavonoids, polyphenols and polysaccharides [3,4]. Among these, *Alpinia oxyphylla* fructus polysaccharide (AOF) is a significant active component, primarily composed of monosaccharides such as arabinose, glucose, and galactose,

and exhibits a range of biological activities [5], including anti-inflammation, antidiuresis and alleviation of Alzheimer's disease symptoms [4,6,7]. Despite this, current research on AOF predominantly focuses on structural characterization and biological activity assessment, with a dearth of theoretical underpinnings for its application in food systems. Therefore, systematically investigating the interactions between AOF and food-based components is of significant importance for expanding the application of AOF and AOF.

Corn starch (CS), extensively utilized as a thickener and texture modifier in the food and chemical industries, faces significant limitations in high-value product development due to its inadequate shear resistance, thermal instability, and susceptibility to retrogradation [8,9]. During gelatinization, starch granules swell and rupture, releasing amylose, which forms a crystalline structure upon cooling, causing retrogradation. This significantly increases the hardness of chilled foods

\* Corresponding authors.

E-mail addresses: [dx335@bath.ac.uk](mailto:dx335@bath.ac.uk) (F. Xie), [peichen@scau.edu.cn](mailto:peichen@scau.edu.cn) (P. Chen).

<https://doi.org/10.1016/j.ijbiomac.2025.143284>

Received 29 November 2024; Received in revised form 30 March 2025; Accepted 16 April 2025

Available online 18 April 2025

0141-8130/© 2025 The Authors. Published by Elsevier B.V. This is an open access article under the CC BY license (<http://creativecommons.org/licenses/by/4.0/>).

like pudding, compromising palatability and commercial value [10]. Recent studies have explored polysaccharide-starch composites systems to enhance starch physicochemical properties. For instance, *Qingke*  $\beta$ -glucan and *Tremella fuciformis* polysaccharide significantly improved starch thermal stability by inhibiting granule swelling and amylose leaching [11,12]. Sodium alginate and soluble soybean polysaccharide effectively delay the aging of wheat starch gels through competitive hydration [13]. Additionally, polysaccharides from *Epiphyllum oxypetalum* (DC.) Haw polysaccharide enhanced tapioca starch physicochemical properties, reducing the hardness of taro balls while improving their freeze-thaw stability and color [14]. Furthermore, AOFP has been shown to exhibit excellent antioxidant activity, and polysaccharides rich in galacturonic acid, such as *Ficus pumila* Linn. polysaccharide, significantly enhanced the antioxidant capacity of starch [4,15]. These results confirm that combining polysaccharides with starch is an efficient approach to improve the stability and functional properties of starch-based food products. Based on these findings, it is hypothesized that AOFP can enhance the gelatinization and retrogradation behavior of corn starch through intermolecular interactions, thereby improving the texture and mouthfeel of foods.

Thus, this study was dedicated to examining the effects of AOFP on the gel characteristics, structural features, and functional activities of CS. By analyzing the impacts of AOFP on the microstructure of CS (including the gel network and crystalline structures) as well as its macroscopic properties (such as thermal stability, rheological properties, and texture), the potential interaction mechanisms between AOFP and corn starch are elucidated. The findings of this research will provide a theoretical foundation for the application of AOFP in starch-based functional food systems.

## 2. Materials and methods

### 2.1. Materials

Native CS (amylose  $26.34 \pm 0.03$  %, w/w) was sourced from COFCO Haiyou Co., Ltd. (Beijing, China). AOF, obtained from Bagueo Sheng Food Co., Ltd. (Guangdong, China), was dried and ground into a powder form. Papain (800 U/mg) and glucoamylase (100 U/mg) were procured from Yuanye Biotechnology Co., Ltd. (Shanghai). The supplier of  $\alpha$ -Amylase ( $\geq 5$  U/mg) was sourced from Sigma-Aldrich (USA). The chemicals employed in this study, aside from the aforementioned, were all of analytical grade.

### 2.2. Extraction of AOFP and chemical components determination

#### 2.2.1. Extraction of AOFP

To extract AOFP using an aqueous method followed by alcohol precipitation, a modified approach based on the technique detailed by Yang et al. [5] was utilized. In this process, AOF powder was combined with distilled water in a 1:12 (w/v) ratio and heated ( $90$  °C, 1 h); this extraction was performed twice. Post-extraction, the mixture underwent centrifugation at 4500 rpm for 10 min to obtain the supernatant. The supernatant was then subjected to reduced pressure concentration at  $55$  °C, followed by the gradual addition of pre-chilled 95 % ethanol to achieve a volume fraction of 75 %. To promote precipitation, the solution was allowed to sit at  $4$  °C for 12 h. The precipitate, redissolved at  $55$  °C, underwent deproteinization using a combination of papain treatment (0.5 % w/v, at  $55$  °C for 2 h) alongside the Sevage method. The sample was subsequently dialyzed at  $4$  °C for 72 h (14 kDa). The resultant solution was freeze-dried ( $-55$  °C) to obtain AOFP, which was stored in a food-grade bag ( $15 \times 22$  cm) at  $4$  °C in the dark. The extraction procedure of AOFP is depicted in Fig. 1.

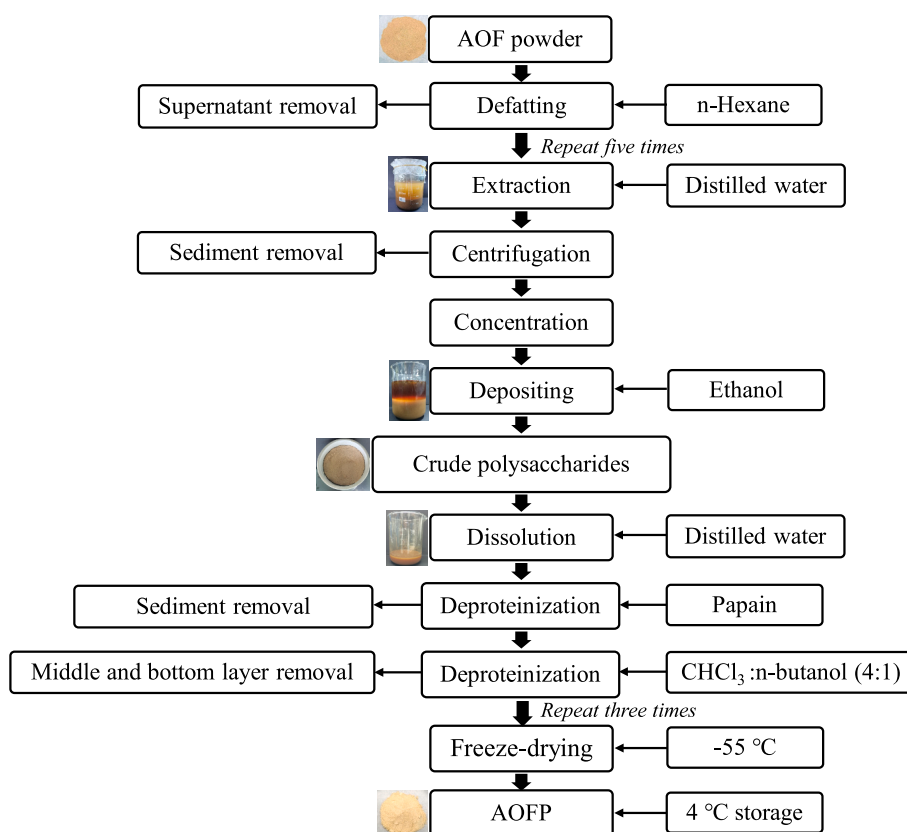


Fig. 1. Flowchart of the extraction process for AOFP.

### 2.2.2. Chemical characterization of AOFP

The phenol-sulfuric acid method was used to determine the overall sugar content in AOFP; the carbazole-sulfuric acid assay was employed to quantify the galacturonic acid levels. And the protein content was assessed using the Coomassie Brilliant Blue method [4].

### 2.2.3. Molecular weight

AOFP's molecular weight was assessed through high-performance gel permeation chromatography (LC-20A, Shimadzu Scientific Instruments, JPN) [5]. The chromatographic separation was conducted on a TSKgel GMPWXL aqueous gel chromatography column (8  $\mu\text{m}$ , 300  $\times$  7.5 mm), and detection was carried out using a RID-20 refractive index detector. The chromatographic conditions were set as follows: mobile phase consisting of 0.1 M  $\text{NaNO}_3$  and 0.05 %  $\text{NaN}_3$  in deionized water, and a flow rate of 0.6 mL/min at 35  $^\circ\text{C}$ . Pullulan polysaccharide standard samples (1.307, 2.178, 96.256, 317.948, 1263.082 kDa) and ZP samples (5 mg/mL) were prepared, and the resulting curves were analyzed to obtain the average molecular weight.

### 2.2.4. Monosaccharide composition analysis

The monosaccharide composition analysis in AOFP was adapted from the methodology established by Yang et al. [5]. Specifically, AOFP (5 mg) underwent acid hydrolysis with 3.0 mL of 2 M TFA (120  $^\circ\text{C}$ , 4 h), and the hydrolysis products were dried under  $\text{N}_2$ . The polysaccharide sample was finally re-dissolved in water, yielding a solution of 50  $\mu\text{g}/\text{mL}$  for further analysis. The sample (20  $\mu\text{L}$ ) was analyzed using a HPLC system (LC-20AD, Shimadzu Scientific Instruments, Japan) equipped with an Xtimate C18 column (5  $\mu\text{m}$ , 200  $\times$  4.6 mm) and an electrochemical detector. The mobile phase consisted of a blend of 0.05 M potassium dihydrogen phosphate solution (pH adjusted to 6.7 with NaOH) and acetonitrile (83:17, v/v), was pumped at a flow rate of 1.0 mL/min at 30  $^\circ\text{C}$ .

### 2.2.5. Thermogravimetric analysis (TGA)

AOFP was characterized utilizing thermogravimetric analysis (Netzsch STA 449 F3/F5, Germany) [16]. A precisely measured 5 mg sample was heated within  $\text{N}_2$  atmosphere (30–800  $^\circ\text{C}$ , 10  $^\circ\text{C}/\text{min}$ ), with mass changes of the polysaccharide meticulously recorded throughout the process.

### 2.3. Preparation of corn starch/AOFP pastes and freeze-dried gel samples

Appropriate amounts of AOFP were weighed based on CS dry weight ratios of 1 %, 2 %, 4 %, and 6 % (w/w), and CS was added. An 8 % (w/w) starch suspension was prepared using distilled water. The resulting CS-AOFP composite systems were designated as CS-1%AOFP, CS-2%AOFP, CS-4%AOFP, and CS-6%AOFP, respectively. A control group was established using a CS sample that did not receive the addition of AOFP.

For the preparation of starch pastes, CS suspensions, both with and without the addition of AOFP, were gelatinized in 250 mL flasks (95  $^\circ\text{C}$ , 30 min), followed by cooling to 25  $^\circ\text{C}$  to achieve complete gelatinization. Fresh and retrograded samples, stored at 4  $^\circ\text{C}$  for 7 days, underwent freeze-drying to produce dried starch gel specimens (Fig. 2).

### 2.4. Rheological properties

Starch pastes (8 %, w/w) were precisely prepared and fully gelatinized according to the procedure in Section 2.3. Upon cooling to 25  $^\circ\text{C}$ , the rheological properties were measured using a rheometer (MCR 502, Anton Paar, Germany), equipped with a parallel-plate (diameter 40 mm, gap 1 mm) [17].

The steady-state viscosity of the 8 % (w/w) starch pastes was measured under a 1 % strain, with shear rates ranging from 0.1 to 100  $\text{s}^{-1}$ . The data were then fitted and analyzed using the power law model as shown in Eq. (1).

$$\tau/\dot{\gamma} = \eta = K\dot{\gamma}^{n-1} \quad (1)$$

where  $\tau$  represents the shear stress (Pa),  $\dot{\gamma}$  represents the shear rate ( $\text{s}^{-1}$ ),  $K$  represents the consistency coefficient ( $\text{Pa}\cdot\text{s}^n$ ),  $n$  represents the flow behavior index, and  $\eta$  is apparent viscosity ( $\text{Pa}\cdot\text{s}$ ).

To investigate the dynamic mechanical properties of starch pastes, including the storage modulus ( $G'$ ), loss modulus ( $G''$ ), and loss factor ( $\tan \delta = G''/G'$ ), a frequency sweep was conducted. The experiment was performed with a constant strain of 1 %, scanning over an angular frequency range from 0.1 to 20 rad/s.

### 2.5. Thermal properties

The heat-absorption pasting behavior of starch samples was evaluated using DSC (DSC4000, PerkinElmer, USA), adhering a protocol from prior research [18]. The onset temperature ( $T_o$ ), peak temperature ( $T_p$ ), and conclusion temperature ( $T_c$ ) were determined via DSC thermography. Specifically, mixtures of CS-AOFP (3.0 mg) and distilled water (9.0  $\mu\text{L}$ ) were prepared, sealed within aluminum pans, and equilibrated at 4  $^\circ\text{C}$  for 12 h to achieve moisture equilibrium. The samples were heated within  $\text{N}_2$  atmosphere (20–100  $^\circ\text{C}$ , 10  $^\circ\text{C}/\text{min}$ ). A control was established using an empty aluminum pan. Following the initial scan, samples were refrigerated at 4  $^\circ\text{C}$  for 7 days to being rescanned under identical conditions. The enthalpy of gelatinization ( $\Delta H_g$ ) and retrogradation ( $\Delta H_r$ ) were quantitatively assessed from the initial and reheating curves, respectively. The calculation of the percentage of retrogradation after 7 days (%) was performed utilizing Eq. (2):

$$R\% = \frac{\Delta H_r(\text{J/g})}{\Delta H_g(\text{J/g})} \times 100\% \quad (2)$$

where  $\Delta H_r$  is the retrogradation enthalpy change (J/g),  $\Delta H_g$  is the gelatinization enthalpy change (J/g).

### 2.6. Gel hardness

The hardness of starch hydrogels was measured utilizing a texture analyzer (EZ-SX 500 N, Shimadzu, Japan) [17]. Freshly prepared starch pastes (8 %, w/w) were placed into plastic cylinder molds (60  $\times$  24 mm), cooled at 25  $^\circ\text{C}$  for 2 h, and then stored at 4  $^\circ\text{C}$  for various durations (0, 1, 3, 5, and 7 days). A cylindrical probe with a diameter of 1.27 cm (P/0.5) was utilized to compress the samples at 1.0 mm/s until a distance of 10.0 mm was achieved, corresponding to a strain of 50 %, with the

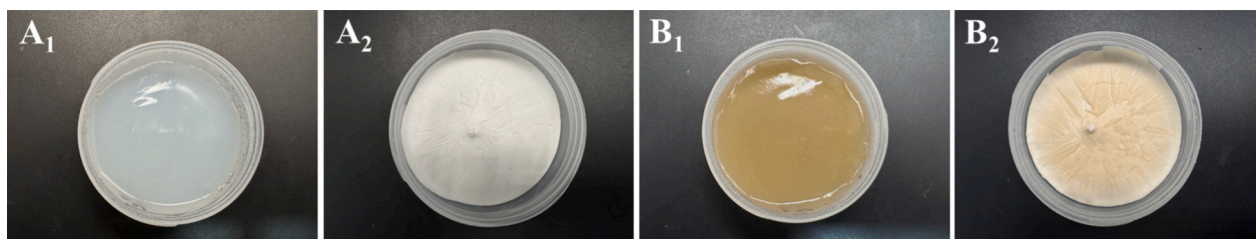


Fig. 2. The freshly prepared CS and CS-6%AOFP starch pastes at 95  $^\circ\text{C}$  for 30 min ( $A_1$  and  $B_1$ ); the freeze-dried samples of the CS and CS-6%AOFP gels ( $A_2$  and  $B_2$ ).

trigger force adjusted to 5.0 g. The hardness parameters were obtained using Texture Exponent Lite software.

## 2.7. Water-holding capacity (WHC)

The water-holding capacity (WHC) of starch hydrogels was evaluated employing the method by Lan et al. [17]. Approximately 10 g of starch hydrogels (8 %, w/w) were placed in centrifuge tubes (50 mL) and stored at 4 °C for 0, 1, 3, 5, and 7 days. Subsequently, the samples were centrifuged at 3000 rpm for 15 min. The remaining gels in the filter cartridge were weighed, following which the supernatant was discarded. The WHC was calculated using Eq. (3):

$$\text{WHC}\% = \frac{\text{Weight of the gel after centrifugation (g)}}{\text{Total weight of the gel before centrifugation (g)}} \times 100\% \quad (3)$$

## 2.8. Iodine-binding capacity

The method of Kong et al. [15] was referenced with some modifications. Fresh starch pastes (1 %, w/v) were following the protocol outlined in Section 2.3. Specifically, a mixture of 100  $\mu\text{L}$  CS-AOFP sample, 4.8 mL distilled water, and 100  $\mu\text{L}$  iodine solution (0.08 %  $\text{I}_2$  and 0.80 % KI, w/v) was prepared and incubated at 25 °C in the dark for 15 min. The spectra were measured using a UV-visible spectrophotometer (Thermo, Waltham, MA, USA) between 350 and 800 nm.

## 2.9. X-ray diffractometry (XRD)

An X-ray diffractometer (Bruker D8 Advance, Bruker AXS Inc., Germany) operated at 40 kV and 40 mA was utilized to analyze the lyophilized hydrogel samples. The powdered samples were evenly spread on the sample holder and subjected to an XRD scan across a  $2\theta$  range from 4 to 40° at 2°/min to acquire XRD diffractograms. The relative crystallinity (RC) was analyzed utilizing MDI Jade 6.0 software, by the method described in our prior paper [17].

$$\text{RC}\% = \frac{A_c}{A_c + A_a} \times 100\% \quad (4)$$

where  $A_c$  and  $A_a$  denote the crystalline and amorphous regions, respectively.

## 2.10. Fourier-transform infrared (FTIR) spectroscopy

In accordance with our previous research [17], we conducted FTIR analysis to obtain the infrared spectra of lyophilized hydrogel samples within a wavenumber range of 650–4000  $\text{cm}^{-1}$  with a resolution of 2  $\text{cm}^{-1}$  using a spectrometer (Nicolet 6700, Thermo Electric Corporation, Waltham, MA, USA). The Fourier-transform infrared spectra between 800 and 1200  $\text{cm}^{-1}$  were deconvoluted using OMNIC software, and the absorbance ratios at 1047  $\text{cm}^{-1}$  to 1022  $\text{cm}^{-1}$  ( $R_{1047/1022}$ ) were calculated.

## 2.11. Scanning electron microscopy (SEM)

The cross-sectional morphology of freeze-dried hydrogel samples was examined using a scanning electron microscope (Hitachi TM4000Plus, Tokyo, Japan) operated at 5 kV and 500 $\times$  magnification, after sputter-coated with gold [17].

## 2.12. Antioxidant capacity of composite gels

### 2.12.1. ABTS<sup>+</sup> radical scavenging activity

The ABTS<sup>+</sup> radical scavenging activity of the samples was studied based following a previously reported method [15]. The freeze-dried hydrogel samples (400 mg) were dissolved in deionized water (5 mL)

to form a homogeneous solution dissolved. The test solution (1 mL) was mixed with ABTS<sup>+</sup> solution (3 mL), subsequently incubated in darkness at 25 °C for 6 min, and centrifugated (4500 rpm, 10 min) to separate the supernatant. Absorbance of the supernatant was measured at 734 nm using a UV-vis spectrophotometer (GENESYS 50, Thermo Fisher Scientific, China). The scavenging activity was calculated as follows:

$$\text{Scavenging ability}\% = \frac{A_0 - A_1}{A_0} \times 100\% \quad (5)$$

where  $A_0$  refers to the absorbance of the control group, where distilled water is utilized as a substitute for the supernatant. Meanwhile,  $A_1$  signifies the absorbance value of the sample group.

### 2.12.2. DPPH radical scavenging activity

The assay procedure for DPPH radical scavenging activity was adapted from the literature with minor modifications [15]. A 1 mL aliquot of the test solution was combined with 4 mL of DPPH solution (1  $\times 10^{-4}$  mol/L) to achieve homogeneity, incubated in the dark at 25 °C for 30 min, and centrifuged to isolate the supernatant. The absorbance of the supernatant was measured at 517 nm (model GENESYS 50, Thermo Fisher Scientific, China). The calculation formula was as follows:

$$\text{Scavenging ability}\% = 1 - \frac{A_1 - A_2}{A_0} \times 100\% \quad (6)$$

where  $A_0$  is defined as the absorbance of the blank control, where ethanol is used in lieu of the supernatant.  $A_1$  denotes the absorbance of the sample group, and  $A_2$  represents the absorbance when ethanol is employed to replace the DPPH-ethanol solution.

## 2.13. In vitro digestibility

Referring to the methodology of Su et al. [19], 2 mg of  $\alpha$ -amylase and 20 mg glucoamylase were combined with 5 mL sodium acetate buffer (0.2 M, pH 6.0) to prepare a mixed enzyme solution. A 5 mL of the enzymatic mixture was added to 10 mL of fully gelatinized starch paste (1 %, w/w), and the enzymatic hydrolysis process was performed in a water bath shaker (37 °C, 160 rpm/min). At 0, 20, and 120 min post-reaction initiation, 0.1 mL of hydrolysate was accurately sampled and immediately mixed with 0.75 mL of anhydrous ethanol to deactivate the enzymes. The digested samples were centrifuged (4000 rpm, 10 min), and the supernatant was collected for further analysis.

The glucose content was measured using a glucose assay kit. Transferred 2.5  $\mu\text{L}$  supernatant to a 96-well plate, mixed with 250  $\mu\text{L}$  the assay reagent, and incubated (37 °C, 10 min). Measured absorbance at 505 nm using an enzyme-labeled instrument (VersaMax, Molecular Devices). The equations for calculating the contents of rapidly digestible starch (RDS), slowly digestible starch (SDS), and resistant starch (RS) were as follows:

$$\text{RDS}\% = (G_{20} - F) \times \frac{0.9}{T} \times 100\% \quad (7)$$

$$\text{SDS}\% = (G_{120} - G_{20}) \times \frac{0.9}{T} \times 100\% \quad (8)$$

$$\text{RS}\% = 1 - (\text{RDS}\% + \text{SDS}\%) \quad (9)$$

where  $F$  represents the free glucose mass at 0 min;  $T$  denotes the total dry weight of CS;  $G_{20}$  and  $G_{120}$  signify the glucose masses measured after 20 and 120 min of digestion.

## 2.14. Statistical analysis

At least triplicate experiments were performed, with the mean  $\pm$  standard deviation being expressed. Duncan's multiple tests in SPSS 22.0 software were employed for statistical analysis to detect significant

**Table 1**  
Chemical composition analysis and molecular weight of *Alpinia oxyphylla* fructus polysaccharide (AOFP).

Sample	AOFP
Yield (%)	3.14 ± 0.23
Total sugar (%)	69.90 ± 1.30
Uronic acid (%)	35.23 ± 1.44
Protein	0.42 ± 0.11
Molecular weight (kDa)	49.222
Polydispersity ( $M_w/M_n$ )	4.245
Monosaccharide composition (mol%)	
Man	1.02
Rib	0.05
Rha	1.89
GlcA	3.08
GalA	37.05
Glc	32.44
Gal	7.19
Xyl	9.01
Ara	7.87
Fuc	0.40

$M_w$ : weight-average molecular weight;  $M_n$ : number-average molecular weight.

differences ( $p < 0.05$ ).

### 3. Results and discussion

#### 3.1. Characterization of AOFP

The chemical composition and molecular weight of AOFP were detailed in Table 1 and Fig. 3. The yield of AOFP was  $3.14 \pm 0.23\%$ , and

the purity was assessed by determining the total sugar, uronic acid, and protein content. The analytical results indicated that AOFP contains  $69.90 \pm 1.30\%$  total sugar,  $35.23 \pm 1.44\%$  uronic acid, and  $0.42 \pm 0.11\%$  protein. The average molecular weight ( $M_w$ ) of AOFP is 49.222 kDa. The primary monosaccharide constituents of AOFP are GlcA (3.08 mol%), GalA (37.05 mol%), Glc (32.44 mol%), Gal (7.19 mol%), Xyl (9.01 mol%), and Ara (7.87 mol%), indicating a high content of glucuronic acid and galacturonic acid in AOFP.

The absorption band between 3100 and 3700  $\text{cm}^{-1}$  corresponds to O—H stretching vibrations from intermolecular and intramolecular hydrogen bonds, while the band at 2800–3000  $\text{cm}^{-1}$  is attributed to C—H stretching vibrations in free carbohydrates [20]. These two characteristic peaks collectively confirm the compound as a carbohydrate substance. The characteristic peak at 1750  $\text{cm}^{-1}$  is indicative of the C=O stretching vibrations of uronic acids, suggesting that AOFP may be acidic, consistent with monosaccharide analysis results [21]. The strong absorption peak between 1600 and 1653  $\text{cm}^{-1}$  arise from the asymmetric stretching vibrations of the carbonyl C=O, and the weak peak at 1420  $\text{cm}^{-1}$  corresponds to the C—O stretching vibrations of the carbonyl group [4]. The absorption peaks in the range of 1000–1200  $\text{cm}^{-1}$  arise from C-O-H and C-O-C stretching vibrations, signifying the existence of pyranose ring structures in the main chain [22,23]. A characteristic absorption peak at 918  $\text{cm}^{-1}$  corresponds to the  $\beta$ -anomeric carbon, while peaks near 830 and 770  $\text{cm}^{-1}$  indicate the presence of  $\alpha$ -glycosidic bonds and pyranose ring structures, respectively, in the polysaccharide [21]. The comprehensive analysis of the infrared spectrum suggests that the obtained polysaccharide is linked through  $\alpha$ - and  $\beta$ -glycosidic bonds, with the sugar rings being pyranose structures.

Fig. 4 presented the TGA and DTG curves of AOFP, indicating two

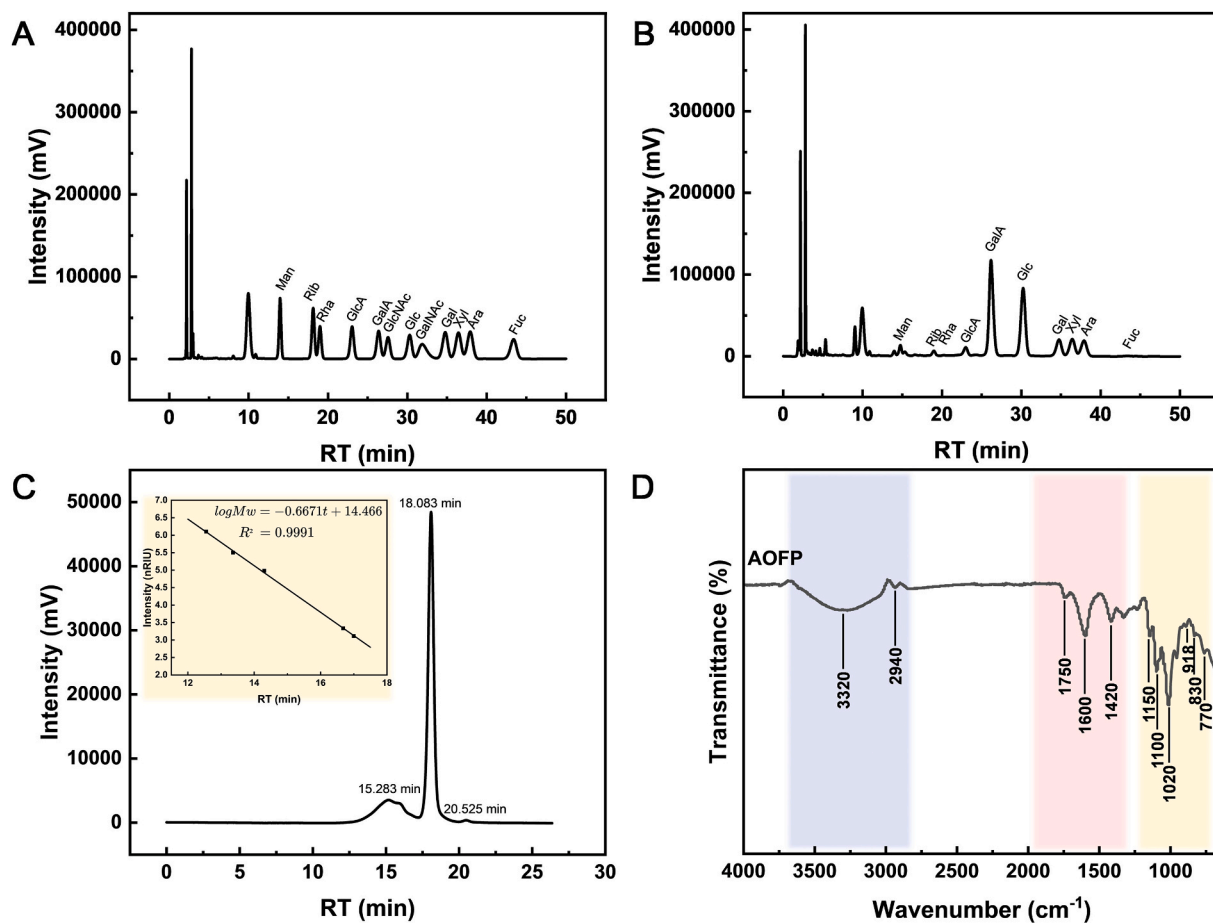


**Fig. 3.** Monosaccharide standards (A); Monosaccharide composition of *Alpinia oxyphylla* fructus polysaccharide (AOFP) (B); Molecular weight distribution of AOFP with the calibration curve of standards with different molecular mass in the inset; (C); FTIR spectrum of AOFP (D).

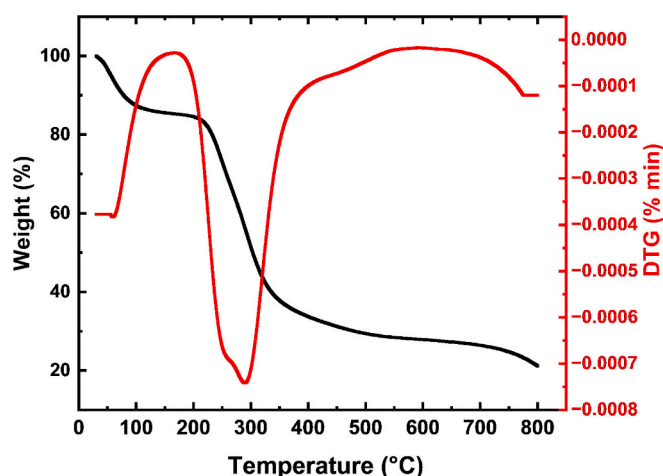


Fig. 4. The thermogravimetric analysis (TGA) and differential thermogravimetric (DTG) curves of AOPF polysaccharide.

distinct thermal degradation stages. The first stage (30–200 °C) involved a 14.76 % attributed to water evaporation. The second stage (200–800 °C) showed a 64.0852 % mass loss, mainly from polysaccharide backbone decomposition. The DTG peak at 290 °C marked the peak degradation rate. Post-290 °C, mass loss slowed, likely due to residual carbon oxidation [24]. The sample's final residue was 21.1550 %. TGA/DTG analysis confirmed that AOPF exhibited good thermal stability below 200 °C.

### 3.2. Gel properties

#### 3.2.1. Steady shear rheological properties

Fig. 5A illustrates the steady-state rheological behavior of CS pastes with varying amounts of AOPF added. As depicted, an increase in shear rate resulted in a rise in shear stress and a decrease in apparent viscosity across all samples, indicative of shear-thinning behavior characteristics [25]. Furthermore, the apparent viscosity of CS paste containing AOPF was generally lower than that of the control CS paste without AOPF. With increasing AOPF content, the apparent viscosity of the CS pastes progressively diminished. The dispersion of AOPF around starch

granules, which reduces water absorption by the granules and thus restricts its swelling, may be responsible for this trend, which results in reduced viscosity within the system [24]. Additionally, the interaction between AOPF and amylose inhibits the leaching of amylose [26]. The analysis of iodine-binding capacity is corroborated by these observations, further confirming the regulatory influence of AOPF on the rheological properties of CS pastes.

The parameters derived from the power law model were summarized in Table 2. In the table,  $R^2 > 0.98$  indicates that the rheological characteristic curves for all samples fit well [25]. The flow behavior indices ( $n$ ) were lower than 1 for all samples, suggesting that all samples exhibited pseudoplastic and shear-thinning characteristics. Kim et al. [27] observed comparable outcomes in the rheological properties of sweet potato starch/*Eucommia ulmoides* leaf powder mixtures. Compared to pure CS gels, the consistency ( $K$ ) and apparent viscosity of the composites decreased with increasing addition of AOPF, further confirming the effect of AOPF in reducing the viscosity and enhancing the fluidity of CS pastes. The impact of AOPF on amylose molecule aggregation may weaken the gel structure [28].

#### 3.2.2. Dynamic rheological properties

The variation in  $G'$  is recognized as an effective criterion for assessing starch gels gelatinization and short-term retrogradation. Notably, the  $G'$  values for all samples significantly exceeded the  $G''$  values, confirming their viscoelastic properties and solid-like behavior, characteristics of weak gel systems [29]. As the angular frequency increased from 0.1 to 20 rad/s, both  $G'$  and  $G''$  demonstrated an increasing trend (Fig. 5B and C). The minimum values occurred at a 6 % AOPF concentration, which corresponded to the measured gel hardness. In alignment with this observation, Wu et al. [26] also observed a decrease in the  $G'$  and  $G''$  values of *Cyperus esculentus* starch as the concentration of *Cyperus esculentus* polysaccharide increased. The decrease in elasticity is probably due to the interaction between AOPF and leached starch molecules, which hindered the aggregation and rearrangement of amylose [28].

Loss tangent ( $\tan \delta$ ) is a significant parameter for assessing gel behavior,  $\tan \delta < 1$  indicates elastic dominance and  $\tan \delta > 1$  reflects viscous dominance [30]. As shown in Fig. 5D, the  $\tan \delta$  values of all gels were  $< 1$ , confirming that they were predominantly elastic weak gels. At the same angular frequency ( $\omega$ ), the  $\tan \delta$  of CS-AOPF composite gels rose as the concentration of AOPF increased, indicating a reduction in intermolecular associations within the starch, and the starch gel containing AOPF exhibited a more pronounced liquid-like behavior (Fig. 5D). These findings obtained align with the investigation conducted by Kong et al. [28], which revealed that CPS resulted in an increase in  $\tan \delta$  for wheat starch. Therefore, it can be inferred that the impact of AOPF on the gelation of CS is primarily on the aspect of elasticity, as AOPF can suppress the ability of CS granules to form a continuous network structure. Since the main polymer forming the crosslinked network is amylose [31], it can be speculated that the interaction of AOPF with leached amylose led to a reduction in amylose-amylose interactions, delaying the re-aggregation of amylose and hindering the formation of an elastic gel [32]. This interference ultimately diminished the gel's overall elasticity and stiffness, aiding in the retention of moisture within the starch gel and yielding a softer texture.

#### 3.2.3. Thermal properties

The thermal properties of the samples were presented in Table 3. Throughout the heating process, the gelatinization phenomenon of the starch slurry delineated a structural transition from a highly ordered state to an amorphous configuration [33]. Comparative analysis with the blank control group, which did not receive AOPF supplementation, revealed a significant increase in  $T_0$ ,  $T_p$ , and  $T_c$  of the samples. Notably, the increments in  $T_p$  and  $T_c$  were particularly pronounced ( $p < 0.05$ ), correlating positively with the escalating concentration of AOPF. The introduction of AOPF induced an upward shift in the gelatinization temperatures of the CS-AOPF system, indicating a potential capacity of

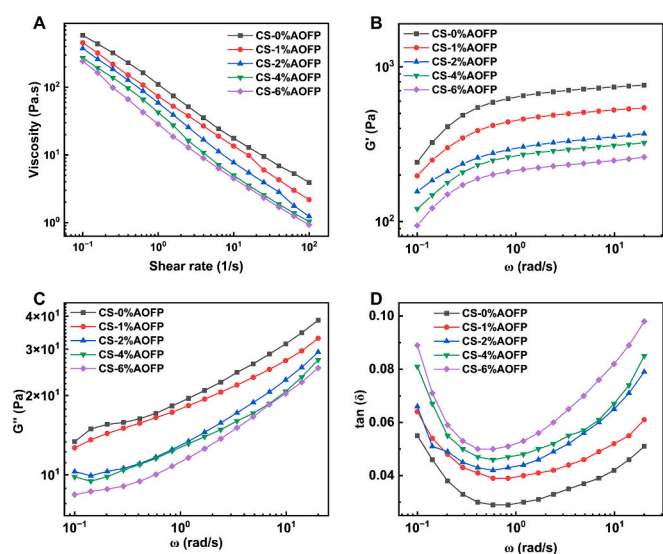


Fig. 5. Viscosity vs. shear rate curves for corn starch (CS) pastes (8 %, w/w) incorporating different contents of *Alpinia oxyphylla* fructus polysaccharide (AOPF) (A); Storage modulus ( $G'$ ) (B), loss modulus  $G''$  (C), and loss factor ( $\tan \delta$ ) (D) vs. angular frequency ( $\omega$ ) curves for CS and CS-AOPF gels.

**Table 2**

Steady-shear rheological results of corn starch (CS) pastes incorporating different contents of *Alpinia oxyphylla* fructus polysaccharide (AOFP).

Sample	$K$ (Pa·s <sup>n</sup> )	$n$	$R^2$
CS	116.80 ± 1.00 <sup>a</sup>	0.26 ± 0.03 <sup>a</sup>	0.999 <sup>a</sup>
CS-1%AOFP	73.34 ± 1.10 <sup>b</sup>	0.21 ± 0.01 <sup>b</sup>	0.999 <sup>a</sup>
CS-2%AOFP	58.63 ± 1.56 <sup>c</sup>	0.20 ± 0.01 <sup>b</sup>	0.998 <sup>a</sup>
CS-4%AOFP	33.08 ± 4.94 <sup>d</sup>	0.09 ± 0.02 <sup>c</sup>	0.999 <sup>a</sup>
CS-6%AOFP	28.38 ± 0.06 <sup>d</sup>	0.08 ± 0.01 <sup>c</sup>	0.999 <sup>a</sup>

Different superscripts in the same column mean significantly different ( $p < 0.05$ ).

AOFP to delay the gelatinization of starch. This phenomenon may be attributed to the disruption of hydrogen bonds within the amorphous and crystalline areas of starch under hydrothermal treatment conditions, while non-starch polysaccharides may hinder water diffusion into the amorphous regions or compete with starch for hydration [33,34]. This competitive effect limited the rate at which water molecules entering starch granules during gelatinization, subsequently restraining their swelling and ultimately resulting in an elevated gelatinization temperature [30,35].

The enthalpy change of gelatinization ( $\Delta H_g$ ) is a pivotal parameter for quantifying the energy required for starch molecules to gelatinize, primarily indicative of the disintegration of starch molecular double helices and the melting of its crystalline structures. The incorporation of AOFP into CS markedly reduced  $\Delta H_g$  in comparison to pure CS (Table 3), with a pronounced downward trend as the concentration of AOFP increased. This finding suggested that AOFP significantly diminished the  $\Delta H_g$  in the polysaccharide-starch matrix, thereby influencing intramolecular starch interactions, a phenomenon corroborated by the literature on the impact of laminaria and *Tremella fuciformis* polysaccharide on starch's  $\Delta H_g$  [12,18]. The reason for this phenomenon could be linked to the interference with double helices in both crystalline and amorphous domains of starch granules, or the incomplete gelatinization of unstable amylose and amylopectin molecules as a result of the heating process [30].

During the retrogradation process, starch molecules transition from a state of disorder to one of order, forming a recrystallized structure [17]. This transition is manifested as an endotherm peak in thermal analysis. As indicated in Table 3, AOFP addition significantly decreased the retrogradation extent of CS after being stored for 7 days. This effect is due to hydrogen bonding interactions between AOFP and starch molecules, which limit the recrystallization process of both amylose and amylopectin. In other words, the physically protective effect of AOFP delays the expansion of starch granules, collectively influencing the retrogradation behavior of starch [36].

### 3.2.4. Gel hardness

Gel hardness serves as a pivotal metric for assessing the structural development of the gel network and the extent of retrogradation reactions, predominantly influenced by the reformation of hydrogen bonds among amylose and amylopectin chains during retrogradation [37]. As illustrated in Fig. 6A, the hardness of the starch gel across all

samples has been observed to increase progressively with extended storage duration. This incremental rise in hardness is attributed to the reconfiguration of amylose and amylopectin chains throughout storage and cooling, leading to the formation of stable double-helical structures that facilitate starch retrogradation and, consequently, enhance the rigidity of the gel framework [38].

The experimental data indicated that CS gels supplemented with AOFP exhibited lower hardness at all storage time points, suggesting that the incorporation of AOFP may attenuate the aging process of CS gels. This effect intensified progressively with increasing AOFP concentrations from 1 % to 6 % (w/w, based on CS mass). Notably, at the zero-day storage mark, the CS gel with 6 % AOFP addition demonstrated the lowest hardness, corroborating the results from the rheological frequency sweep measurements of  $G'$  and reflecting its short-term retrogradation characteristics. Consistent with previous findings by Chen et al. [14]. The short-term retrogradation inhibition of CS by AOFP likely resulted from disrupted interactions between amylose molecules, which hinder amylose rearrangement and amylopectin recrystallization, ultimately reducing gel hardness [30]. Furthermore, AOFP-water interactions inhibited starch granule swelling, competed with starch for water availability, and suppressed starch chain aggregation [15,32].

After a storage period of 7 days, the hardness of CS gels included with AOFP exhibited a significant decrease. These findings indicate that the incorporation of AOFP significantly altered the textural properties of CS gels during the aging process, leading to a reduction in hardness [17]. This effect may be because that AOFP hinders the entanglement between amylose and amylopectin through steric hindrance, thereby resulting in a looser gel structure [39]. In fact, the aging of starch is a dynamic process involving the migration of water molecules. The hydrophilic nature of polysaccharides allows them to competitively absorb water from starch, reducing the available water for the recrystallization of amylopectin and, consequently, weakening the interactions between amylopectin chains and inhibiting their recrystallization. Furthermore, AOFP interacts with the leached amylose chains, enhancing the enveloping effect on the starch molecule surface, disrupting the intermolecular crosslinking within starch, and delaying the starch recrystallization process, further reducing the hardness of the starch gel [16]. This action

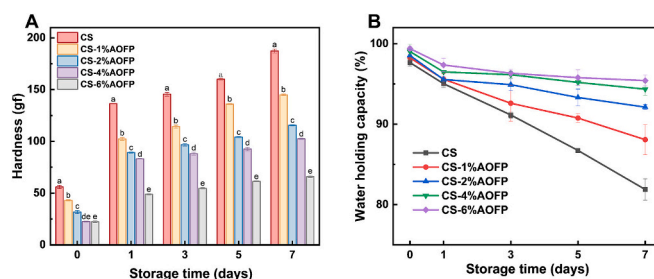


**Fig. 6.** Hardness values (A); Water-holding capacity (B) of corn starch (CS) gels (8 %, w/w) incorporating different contents of *Alpinia oxyphylla* fructus polysaccharide (AOFP) after storage. Statistically significant differences in hardness among samples on the same day are denoted by different letters ( $p < 0.05$ ).

**Table 3**

Thermal properties of corn starch (CS) incorporating different contents of *Alpinia oxyphylla* fructus polysaccharide (AOFP).

Samples	$T_0$ (°C)	$T_p$ (°C)	$T_c$ (°C)	$\Delta H_g$ (J/g)	$R_7$ (%)
0%AOFP-NCS	65.72 ± 0.14 <sup>c</sup>	71.55 ± 0.09 <sup>d</sup>	77.99 ± 0.40 <sup>d</sup>	15.40 ± 0.30 <sup>a</sup>	54.95 ± 1.07 <sup>a</sup>
1%AOFP-NCS	66.66 ± 0.36 <sup>b</sup>	72.66 ± 0.09 <sup>c</sup>	79.33 ± 0.02 <sup>c</sup>	14.31 ± 0.08 <sup>b</sup>	44.50 ± 0.45 <sup>b</sup>
2%AOFP-NCS	66.92 ± 0.01 <sup>b</sup>	72.95 ± 0.02 <sup>b</sup>	80.11 ± 0.16 <sup>b</sup>	14.09 ± 0.01 <sup>b</sup>	39.55 ± 0.27 <sup>c</sup>
4%AOFP-NCS	67.01 ± 0.01 <sup>b</sup>	73.14 ± 0.03 <sup>b</sup>	80.28 ± 0.08 <sup>ab</sup>	13.94 ± 0.01 <sup>b</sup>	35.23 ± 1.15 <sup>d</sup>
6%AOFP-NCS	67.59 ± 0.33 <sup>a</sup>	73.48 ± 0.28 <sup>a</sup>	80.95 ± 0.80 <sup>a</sup>	12.94 ± 0.43 <sup>c</sup>	32.58 ± 1.08 <sup>e</sup>

$T_0$ , onset temperature;  $T_p$ , peak temperature;  $T_c$ , conclusion temperature;  $\Delta H_g$ , enthalpy change;  $R_7$ , percentage of retrogradation on Day 7, namely  $(\Delta H_g / \Delta H_0) \times 100$ . The results, presented in the form of means ± standard deviation, are derived from triplicate measurements. Within each column, varying superscripts denote statistically significant differences ( $p < 0.05$ ).

slows down the rate of starch aging, with significant implications for the texture and stability of starch-based foods [13]. This result is also supported by the lower aging rate ( $R_7\%$ ) and the XRD results.

### 3.2.5. Water-holding capacity (WHC)

WHC serves as a pivotal parameter for assessing the characteristics of starch gels, effectively indicating the extent of starch retrogradation [40]. During food processing and storage, the WHC of starch gels significantly influences their texture and stability, thereby affecting consumer acceptance. As depicted in Fig. 6B, the WHC of all starch gels demonstrated during refrigerated storage, attributable to the aging process that occurred during storage, leading to a denser network structure and increased moisture migration and loss. Notably, gels supplemented with AOPF exhibited a significant enhancement in WHC than native starch gels, indicating that AOPF effectively reduced water migration during gel aging. The enhancement observed can be ascribed to AOPF-starch interactions, which impeded amylose realignment and amylopectin recrystallization, thereby enhancing the WHC of the composite gels [32]. The presence of AOPF diminished the strength of hydrogen bonds within the starch double helices, fundamentally delaying the retrogradation of CS [41]. As a hydrophilic polysaccharide, AOPF can uniformly permeate the starch gel matrix, effectively absorbing and retaining a greater quantity of moisture within the gel matrix, and interacting with starch molecules through hydrogen bonding, which aids in the retention of moisture within the starch gel network [42].

## 3.3. Structural properties

### 3.3.1. Iodine-binding capacity

Fig. 7 delineates the impact of varying AOPF supplementation on the absorption spectrum of the complex formed between CS and iodine. The encapsulation of iodine molecules within the helical cavities of starch, leading to the formation of a colored complex. In this context, the amylose-iodine complex typically displays a blue color with an absorption peak at 540–660 nm, while the amylopectin-iodine complex appears purple, exhibiting a peak at 500–540 nm [43]. The quantity of iodine molecules complexed within starch helical cavities dictates the absorption wavelength of the mixture. Hence, the maximum absorption wavelength of the starch-iodine complex can be indicative of the relative concentration of amylose or amylopectin primarily complexed with iodine in the system [44].

Fig. 7 illustrates a characteristic absorbance peak at 620 nm for the CS-AOPF complex system, indicating a high affinity of iodine for the amylose fraction within CS. With increasing AOPF concentration, the absorption peak, indicative of iodine-binding capacity, progressively decreased, suggesting an increased interaction between AOPF and

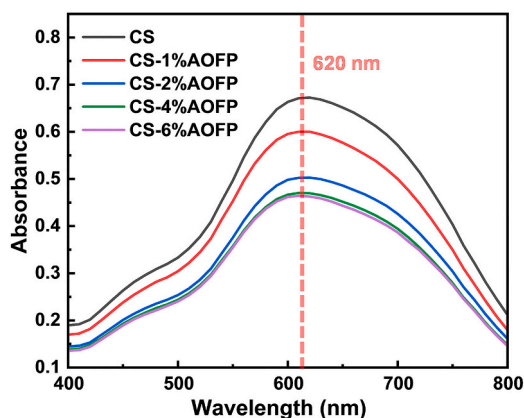


Fig. 7. Effect of *Alpinia oxyphylla* fructus polysaccharide (AOPF) content on the iodine binding capacity of corn starch (CS) pastes (8 % w/w).

amylose. These observations aligned with prior research, which demonstrated that polysaccharides can suppress the formation of starch-iodine complexes through interactions with starch, leading to changes in absorbance [45]. This phenomenon may be attributed to the helical cavities formed by amylose, into which AOPF molecules may enter and bind, forming V-type inclusion complexes, thereby inhibiting the formation of starch-iodine mixtures [15,46]. With an increase in AOPF concentration, the number of inclusion complexes increased, reducing the amount of amylose available for binding with iodine, and consequently lowering the peak absorbance. These results further confirmed that AOPF can bind with extracted amylose and potentially affect the gel structure and properties of starch.

### 3.3.2. XRD

Fig. 8 illustrates the XRD patterns and crystallinity of different starch samples. The XRD pattern of native CS exhibited characteristic peaks of an A-type crystalline structure at  $2\theta$  angles of  $15^\circ$ ,  $17^\circ$ ,  $18^\circ$ ,  $20^\circ$ , and  $23^\circ$  (Fig. 8A) [47]. In contrast, the gelatinized CS, as depicted in Fig. 8B, exhibited a disappearance of the A-type structure's characteristic peaks, replaced by diffraction peaks appearing at  $17^\circ$  and  $20^\circ$ , indicative of a transformation to a B + V type crystalline structure pattern. This alteration is probably a result of the disruption to the ordered structure during gelatinization and its subsequent rearrangement during the aging process [14], as suggested by Zhang et al. [30] and Wang et al. [34]. Furthermore, no noteworthy disparities in the crystal structure of all CS/AOPF mixtures were observed, indicating that AOPF does not affect the crystal structure of the composite gel system (Fig. 8B and C). Zhou et al. [48] observed similar results in their study on the effects of laminarin on wheat starch, indicating that the sugar likely has minimal influence on the crystal structure of starch gels.

The extent of starch retrogradation can be assessed by monitoring changes in crystallinity, as depicted in Fig. 8B and C. The relative crystallinity of starch samples is generally lower than that of untreated native starch, primarily due to thermal disruption of the starch's ordered structure [49]. Increasing AOPF content reduced the relative crystallinity of the samples, indicating that AOPF contributed to the delay of starch retrogradation. This effect may be related to enhanced physical entanglement between AOPF and CS molecules [50]. Interactions between AOPF hydroxyl groups and amylose/amylopectin side chains may interfere with or inhibit the formation of double helices and the recrystallization of branches, thereby affecting the compactness of the gel structure [14,32]. These findings are consistent with previous observations regarding the hardness and WHC of starch gels, further validating the inhibitory role of AOPF on starch retrogradation.

The ratio  $R_{1047/1022}$  represents the absorbance at  $1047\text{ cm}^{-1}$  relative to that at  $1022\text{ cm}^{-1}$ . A significant difference between columns denoted by different letters is indicated by Duncan's test, with a  $p$ -value threshold of Duncan's test ( $p < 0.05$ ).

### 3.3.3. FTIR

FTIR is a conventional analytical technique for investigating functional groups and short-range order within starch. Fig. 9(A and B) shows the FTIR spectra of starch gels in the range of  $4000\text{--}800\text{ cm}^{-1}$ . The absorption peaks between  $3800$  and  $3000\text{ cm}^{-1}$  primarily arise from

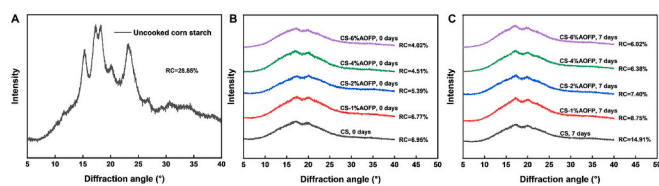


Fig. 8. XRD curves for native corn starch (CS) (A) and gelatinized CS samples incorporating different contents of *Alpinia oxyphylla* fructus polysaccharide (AOPF) after storage at  $4^\circ\text{C}$  for 0 (B) and 7 days (C).

O—H groups stretching vibrations, while the peak at  $2930\text{ cm}^{-1}$  corresponds to  $\text{CH}_2$  antisymmetric stretching vibration [15,51]. According to Xu et al. [52], the intense peak observed at  $1640\text{ cm}^{-1}$  corresponds to O—H bending vibrations of water molecules within the sample. Compared to the control samples without the addition of AOFP, no new characteristic peaks emerged in the spectra of samples with AOFP, indicating the absence of covalent bonds newly formed between AOFP and starch. Upon the incorporation of AOFP, the broadening of the peak at  $3400\text{ cm}^{-1}$  in the starch gel suggested the presence of multi-hydroxyl structures in AOFP [16]. Furthermore, adding AOFP caused a redshift in the  $1640\text{ cm}^{-1}$  absorption peak, implying that AOFP interacted predominantly with starch through hydrogen bonding. This interaction may alter the distribution and state of water molecules within the starch, thereby influencing the properties of the starch gel [14].

The FTIR spectra of starch display a peak at  $1047\text{ cm}^{-1}$  reflecting its crystalline structure, and a peak at  $1022\text{ cm}^{-1}$  indicating its amorphous structure. Table 4 summarizes these absorbance ratios ( $R_{1047/1022}$ ) for starch, reflecting the short-range order inside it, which represents the degree of starch retrogradation [17]. A higher  $R_{1047/1022}$  ratio signifies a greater degree of short-range order and a more compact network structure of the starch gel. The  $R_{1047/1022}$  values for all samples increased with prolonged storage, suggesting that the starch continued to retrograde, with its structural order progressively enhancing during storage. The addition of AOFP to CS resulted in a decrease in  $R_{1047/1022}$  for starch gels to varying degrees (Table 4), indicating that AOFP can effectively suppress the formation of ordered structures during starch retrogradation. This suppression likely results from hydrogen bonding interactions between AOFP and starch molecules, which delays starch chain association and recrystallization, thereby inhibiting short-term retrogradation of CS [36].

### 3.3.4. SEM

Fig. 10 displays SEM images of freeze-dried CS-AOFP composites cross-sections. No intact starch granules were observed in any samples; instead, irregular flake-like and honeycomb structures were evident, indicating complete gelatinization and the formation of a relatively uniform matrix, consistent with previous research findings [53]. The pore formation within the gels was attributed to water sublimation occurring throughout the freeze-drying process. The network structure of CS gels exhibited greater regularity and intensity when compared to CS-AOFP composite gels that incorporated AOFP. At low concentrations of AOFP, the gel network structure was relatively uniform, with a broad distribution of pore sizes. As the AOFP content increased, the uniformity of the gel structure decreased, and the pore sizes and shapes became more irregular, likely due to AOFP-starch interactions disrupting the

orderly arrangement and aggregation of starch molecules [36]. At higher concentrations of AOFP, the porosity of the gel network structure increased, and the pore size distribution broadened, possibly due to AOFP-induced changes in the physical properties of the starch gel, thereby affecting the stability and structural integrity of the gel [54].

As the storage period extends, after being stored for 7 days under refrigeration conditions at  $4\text{ }^\circ\text{C}$ , the entanglement between starch molecules increased, leading to the gradual expulsion of pore water from the gel network, which in turn caused partial destruction and collapse of the starch gel structure [36]. During the retrogradation phase of starch, the incorporation of AOFP hindered the rearrangement and aggregation of amylose and amylopectin, resulting in the deterioration of the gel's network structure and a reduction in the seepage of water molecules [39]. However, the distribution of water molecules within the gel remains uneven. In conjunction with the water retention results shown in Fig. 10, and the interaction between AOFP and water molecules in the composite system, it could be inferred that AOFP functions as a water-retaining agent, thereby enhancing the water retention capacity of the composite system [15,55]. Consequently, during the freeze-drying process, more water molecules were evaporated, resulting in a more relaxed and porous network structure of the gel. Additionally, SEM images at a magnification of  $500\times$  revealed that AOFP adsorption on starch pore surfaces formed fine filamentous crosslinked structures, disrupting the porous network and further reducing gel hardness [16].

### 3.4. Antioxidant capacity of composite gels

The antioxidant properties of the CS-AOFP composite system were evaluated through free radical scavenging assays. DPPH and  $\text{ABTS}^+$ , two widely used methods based on electron-deficient free radical mechanisms, were employed for antioxidant activity determination. The  $\text{ABTS}^+$  assay demonstrated superior performance due to its faster reaction kinetics, higher sensitivity, and reduced interference from sample coloration, enabling more precise detection of subtle concentration variations. Both methods involve reaction mechanisms based on hydrogen atom transfer (HAT) and single electron transfer (SET) [56]. As illustrated in Fig. 11, the antioxidant capacity of the composite gels exhibited a concentration-dependent enhancement with increasing AOFP content. This trend may be attributed to the abundant uronic acids present in AOFP, whose electrophilic groups facilitate the release of hydrogen from O—H bonds [4]. Notably, higher concentrations of galacturonic acids were associated with stronger metal chelating capabilities, thereby inhibiting the efficacy of metal ions in the generation of hydroxyl radicals [57]. Furthermore, the negatively charged polysaccharide molecules may form coordination complexes with metal ions,

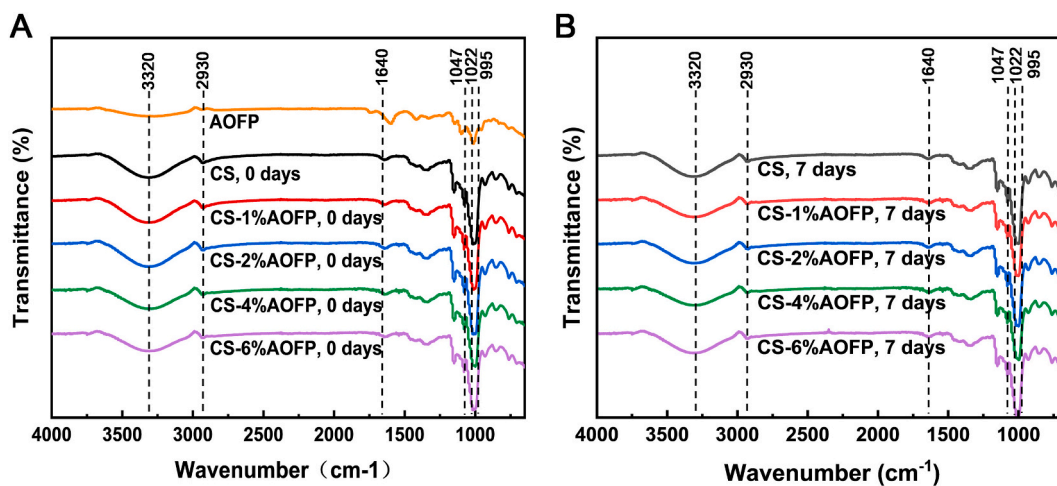
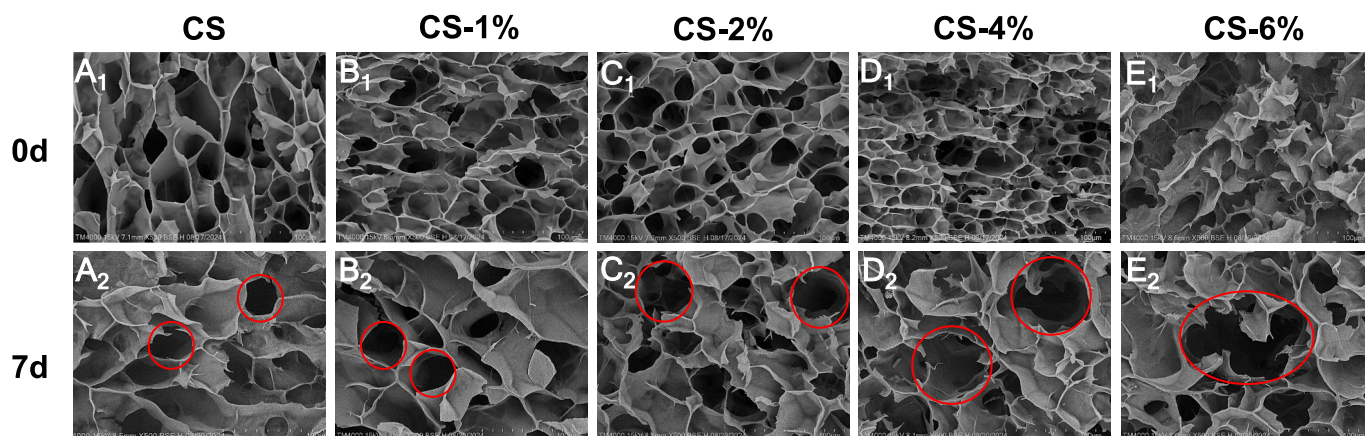
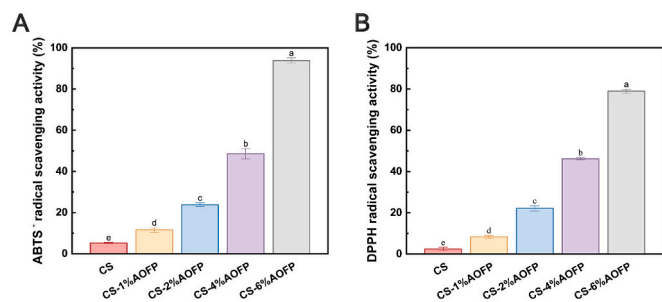


Fig. 9. FTIR spectra of corn starch (CS) gels incorporating different contents of *Alpinia oxyphylla* fructus polysaccharide (AOFP) after storage at  $4\text{ }^\circ\text{C}$  for 0 (A) and 7 days (B).

**Table 4**Peak ratio values from the deconvolution profile of gelatinized corn starch (CS), with varying additions of *Alpinia oxyphylla* fructus polysaccharide (AOFP) content.

Samples	$R_{1047/1022}$ on day 0	$R_{1047/1022}$ on day 7	RC (%) on day 0	RC (%) on day 7
CS	0.966 ± 0.002 <sup>a</sup>	1.038 ± 0.021 <sup>a</sup>	6.950 ± 0.053 <sup>a</sup>	14.910 ± 0.320 <sup>a</sup>
CS-1%AOFP	0.951 ± 0.022 <sup>ab</sup>	0.992 ± 0.004 <sup>b</sup>	6.770 ± 0.166 <sup>a</sup>	8.747 ± 0.076 <sup>b</sup>
CS-2%AOFP	0.939 ± 0.004 <sup>b</sup>	0.983 ± 0.009 <sup>b</sup>	5.390 ± 0.132 <sup>b</sup>	7.403 ± 0.047 <sup>c</sup>
CS-4%AOFP	0.910 ± 0.018 <sup>c</sup>	0.947 ± 0.002 <sup>c</sup>	4.510 ± 0.369 <sup>c</sup>	6.377 ± 0.197 <sup>d</sup>
CS-6%AOFP	0.898 ± 0.010 <sup>c</sup>	0.934 ± 0.005 <sup>c</sup>	4.020 ± 0.061 <sup>d</sup>	6.023 ± 0.142 <sup>e</sup>

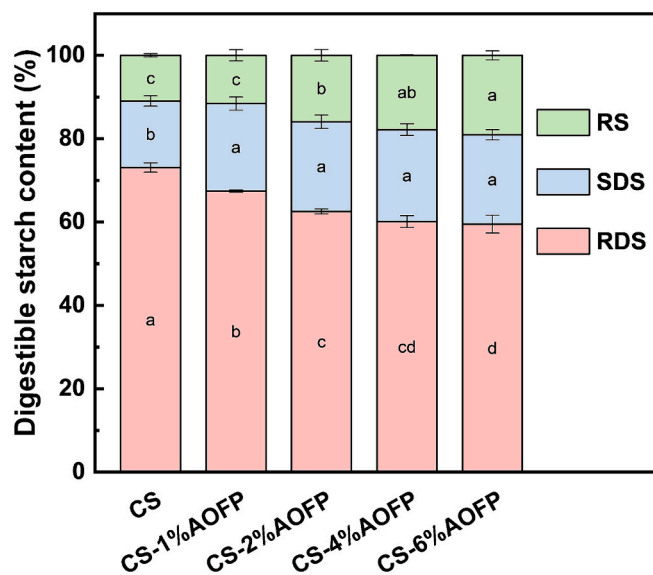
**Fig. 10.** SEM images of corn starch (CS) gels incorporating different contents of *Alpinia oxyphylla* fructus polysaccharide (AOFP). A<sub>1</sub>, B<sub>1</sub>, C<sub>1</sub>, D<sub>1</sub>, E<sub>1</sub>: CS-AOFP after storage at 4 °C for 0 day; A<sub>2</sub>, B<sub>2</sub>, C<sub>2</sub>, D<sub>2</sub>, E<sub>2</sub>: CS-AOFP after storage at 4 °C for 7 days.**Fig. 11.** Antioxidant activity of corns starch (CS) gels incorporating different contents of *Alpinia oxyphylla* fructus polysaccharide (AOFP).

directly scavenging hydroxyl radicals (OH<sup>•</sup>) in the vicinity of the polysaccharide backbone [58].

### 3.5. In vitro digestibility

Starch, serving as a primary energy source for humans, exhibits digestion kinetics that are intricately linked to postprandial glycemic responses and insulin fluctuations [36]. The digestive characteristics of starch are notably affected by various factors, including amylose content, crystallinity, and surface interactions. Classifying starch into RDS, SDS, and RS according to their digestive enzymatic degradation rate, which explains glucose release kinetics and total glucose content under simulated intestinal conditions, offering insights into starch digestion dynamics and glucose metabolism [14].

Fig. 12 illustrates the effect of AOFP concentration on the enzymatic hydrolysis rate of CS. Compared to the control group, elevating AOFP concentration significantly reduced RDS content while markedly increasing SDS and RS contents within the CS-AOFP composite gel. The modulatory effect of AOFP on starch digestibility was likely attributed to its physical barrier mechanism [32]. As shown in Fig. 13, on one hand, AOFP interacted with leached amylose through hydrogen bonding,

**Fig. 12.** Contents of rapidly digestible starch (RDS), slowly digestible starch (SDS), and resistant starch (RS) in corn starch (CS) gels incorporating different contents of *Alpinia oxyphylla* fructus polysaccharide (AOFP) at 25 °C after gelatinization.

resulting in increased steric hindrance [28]. Concurrently, AOFP adhered to the starch granules surface, forming a physical barrier that further restricted the access of enzymes to starch molecules [39,59]. On the other hand, AOFP may be complex with hydrolytic enzymes through molecular adsorption, with its non-competitive inhibitory action facilitating a reduction in starch digestibility [32]. Collectively, these results conclude that AOFP can effectively decrease the digestion rate of starch, potentially exerting a positive influence on the control of postprandial glycemic and insulinemic responses.

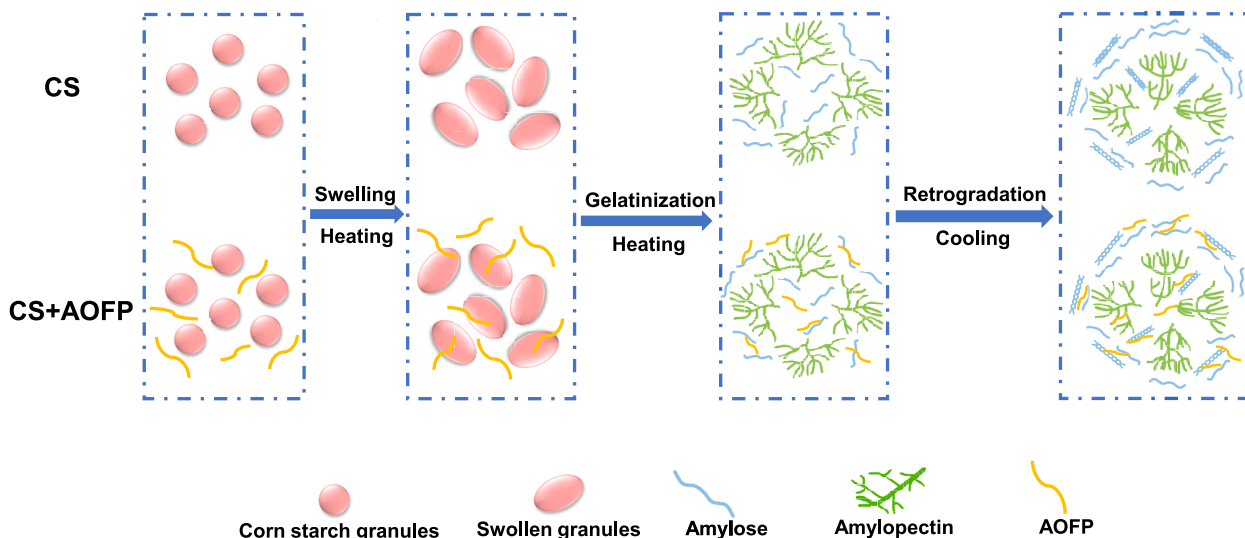


Fig. 13. Schematic representation of the structural changes of corn starch (CS) gels without and with the addition of *Alpinia oxyphyllae* fructus polysaccharide (AOFP).

#### 4. Conclusions

This study assessed the impact of AOFP on the rheological properties, thermodynamic characteristics, textural properties, WHC, structural features, in vitro digestibility, and antioxidant activity of CS. Experimental results demonstrated that AOFP significantly reduced the amylose leaching during gelatinization. FTIR analysis revealed potential hydrogen bonding interactions between AOFP and amylose molecules. The incorporation of AOFP modified the regular network structure of CS gels, enabling its penetration into amylose molecules and creating steric hindrance effects that increased the distance between starch chains. This process weakened the interactions between amylose and amylopectin, consequently retarding starch retrogradation and recrystallization. These findings were supported by thermodynamic analysis, XRD, and FTIR results, demonstrating that the retrogradation rate ( $R_7$ ) of the AOFP-CS system decreased from  $54.95 \pm 1.07\%$  to  $32.58 \pm 1.08\%$ , while the relative crystallinity on day 7 decreased from  $14.910 \pm 0.320\%$  to  $6.023 \pm 0.142\%$ . In the presence of AOFP, both the storage modulus ( $G'$ ) and loss modulus ( $G''$ ) of the gels were reduced, and the hardness decreased from  $187.32 \pm 1.87$  gf to  $66.06 \pm 1.08$  gf. Additionally, the WHC exhibited a slower decline, contributing to improved quality and stability during storage. Furthermore, AOFP enhanced the anti-digestibility and antioxidant activity of CS, with RS content increasing from  $10.96 \pm 0.38\%$  to  $19.08 \pm 1.06\%$ , and ABTS<sup>+</sup> and DPPH radical scavenging activities increasing from  $5.24 \pm 0.23\%$  to  $97.36 \pm 1.12\%$  and from  $1.97 \pm 0.99\%$  to  $89.61 \pm 0.91\%$ , respectively. These findings highlight the potential of AOFP for high-value applications in starch-based food products.

#### CRedit authorship contribution statement

**Zihan Li:** Writing – original draft, Methodology, Investigation, Data curation. **Qingfei Duan:** Methodology. **Yongmei Mo:** Methodology, Conceptualization. **Fuhan Xie:** Visualization, Formal analysis. **Qian Zhou:** Methodology, Investigation. **Pingping Sun:** Methodology, Investigation. **Changfu Lu:** Methodology, Funding acquisition. **Fengwei Xie:** Writing – review & editing, Methodology. **Pei Chen:** Writing – review & editing, Supervision, Funding acquisition, Conceptualization.

#### Declaration of competing interest

The authors declare that they have no known competing financial

interests or personal relationships that could have appeared to influence the work reported in this paper.

#### Acknowledgments

This work was supported by the National Natural Science Foundation of China (Grant No. 32472250) and the Guangdong Basic and the Applied Basic Research Foundation (Grant No. 2024A1515012684). Additionally, this research was supported by the Guangdong Province Modern Agricultural Industry Key Technology R&D Innovation Team Construction Project (Processing and Preservation Key Technologies, Grant No. 2024CXTD16); and the Rural Science and Technology Special Commissioner Program of the “Hundred-Thousand-Million Project” (Grant No. KTP20240142).

#### Appendix A. Supplementary data

Supplementary data to this article can be found online at <https://doi.org/10.1016/j.ijbiomac.2025.143284>.

#### Data availability

Data will be made available on request.

#### References

- [1] Q. Zhang, Y. Zheng, X. Hu, X. Hu, W. Lv, D. Lv, J. Chen, M. Wu, Q. Song, J. Shentu, Ethnopharmacological uses, phytochemistry, biological activities, and therapeutic applications of *Alpinia oxyphylla* Miquel: a review, *J. Ethnopharmacol.* 224 (2018) 149–168.
- [2] G.O.W.A. Yangjiang, Dayaba, *Alpinia oxyphylla* are now in season! Which is your favorite way to enjoy them. <https://mp.weixin.qq.com/s/aPq68bMN-SXYI2tsf8HgXw> (Accessed June 20 2022).
- [3] Y. Liu, R. Wang, X. Hu, C. Yu, Z. Wang, L. Zhang, S. Liu, C. Li, Optimization of ultrasonic extraction of bioactive components from *Alpinia oxyphylla* Fructus using response surface methodology, *J. Appl. Res. Med. Aromat. Plants* 41 (2024) 100557.
- [4] R. Wang, X. Ruan, J. Chen, L. Deng, W. Zhou, X. Shuai, R. Liang, T. Dai, Physicochemical characterization and biological properties of polysaccharides from *Alpinia oxyphylla* fructus, *Polymers* 16 (12) (2024) 1705.
- [5] X. Yang, Y. Yang, H. Chen, T. Xu, C. Li, R. Zhou, L. Gao, M. Han, X. He, Y. Chen, Extraction, isolation, immunoregulatory activity, and characterization of *Alpinia oxyphylla* fructus polysaccharides, *Int. J. Biol. Macromol.* 155 (2020) 927–937.
- [6] Y. Han, J. Wu, Y. Liu, J. Qi, C. Wang, T. Yu, Y. Xia, H. Li, Therapeutic effect and mechanism of polysaccharide from *Alpinia oxyphylla* fructus on urinary incontinence, *Int. J. Biol. Macromol.* 128 (2019) 804–813.

- [7] W. Shi, J. Zhong, Q. Zhang, C. Yan, Structural characterization and antineuroinflammatory activity of a novel heteropolysaccharide obtained from the fruits of *Alpinia oxyphylla*, *Carbohydr. Polym.* 229 (2020) 115405.
- [8] S. Chen, L. Qin, T. Chen, Q. Yu, Y. Chen, W. Xiao, X. Ji, J. Xie, Modification of starch by polysaccharides in pasting, rheology, texture and in vitro digestion: a review, *Int. J. Biol. Macromol.* 207 (2022) 81–89.
- [9] B. Rabeie, N.M. Mahmoodi, Green and environmentally friendly architecture of starch-based ternary magnetic biocomposite (Starch/MIL100/CoFe2O4): synthesis and photocatalytic degradation of tetracycline and dye, *Int. J. Biol. Macromol.* 274 (2024) 133318.
- [10] S.G. Borad, A.A. Patel, A.K. Singh, S.K. Tomar, R.R.B. Singh, Effect of storage and reheating on textural properties of rice in dairy dessert as related to its pasting properties and microstructure, *Lwt* 80 (2017) 485–491.
- [11] L. Zhao, X. Jin, J. Wu, H. Chen, Effects of Qingke  $\beta$ -glucan with different molecular weights on pasting, gelation, and digestive properties of rice starch, *Food Chem. X* 19 (2023) 100803.
- [12] F. Yang, Q. Du, T. Miao, X. Zhang, W. Xu, D. Jia, Interaction between potato starch and *Tremella fuciformis* polysaccharide, *Food Hydrocoll.* 127 (2022) 107509.
- [13] K. Zhao, Z. Jia, L. Hou, S. Xiao, H. Yang, W. Ding, Y. Wei, Y. Wu, X. Wang, Study on physicochemical properties and anti-aging mechanism of wheat starch by anionic polysaccharides, *Int. J. Biol. Macromol.* 253 (2023) 127431.
- [14] N. Chen, Z.-J. Feng, H.-X. Gao, Q. He, W.-C. Zeng, Elucidating effects of *Epiphyllum oxypetalum* (DC.) Haw polysaccharide on the physicochemical and digestive properties of tapioca starch, *Int. J. Biol. Macromol.* 260 (2024) 129446.
- [15] J. Kong, S. Mo, J. Hu, M. Shen, Q. Yu, Y. Chen, J. Xie, Effects of *Ficus pumila* Linn. polysaccharide on physicochemical and digestive properties of corn starch, *Food Biosci.* 58 (2024) 103811.
- [16] W. Fei, L. Rong, X. Qi, X. Chen, Y. Luo, H. Wen, J. Xie, Effects of *Premna microphylla turcz* polysaccharide on rheological, gelling, and structural properties of mung bean starch and their interactions, *Food Res. Int.* 189 (2024) 114561.
- [17] G. Lan, S. Xie, Q. Duan, W. Huang, W. Huang, J. Zhou, P. Chen, F. Xie, Effect of soybean polysaccharide and soybean oil on gelatinization and retrogradation properties of corn starch, *Int. J. Biol. Macromol.* 264 (2024) 130772.
- [18] J. Su, S. He, S. Lei, K. Huang, C. Li, Y. Zhang, H. Zeng, Interaction force between laminarin and different crystal starches describes the gelatinization properties, *Food Hydrocoll.* 147 (2024) 109380.
- [19] H.N. Englyst, S.M. Kingman, J.H. Cummings, Classification and measurement of nutritionally important starch fractions, *Eur. J. Clin. Nutr.* 46 (1992) S33–S50.
- [20] Y. Wang, X. Wei, F. Wang, J. Xu, X. Tang, N. Li, Structural characterization and antioxidant activity of polysaccharide from ginger, *Int. J. Biol. Macromol.* 111 (2018) 862–869.
- [21] Y. Huang, W. Xie, T. Tang, H. Chen, X. Zhou, Structural characteristics, antioxidant and hypoglycemic activities of polysaccharides from *Mori Fructus* based on different extraction methods, *Front. Nutr.* 10 (2023).
- [22] Y. Bu, B. Yin, Z. Qiu, L. Li, B. Zhang, Z. Zheng, M. Li, Structural characterization and antioxidant activities of polysaccharides extracted from *Polygonati rhizoma pomace*, *Food Chem. X* 23 (2024) 101778.
- [23] X.-D. Dong, Y.-Y. Feng, Y.-N. Liu, H.-Y. Ji, S.-S. Yu, A. Liu, J. Yu, A novel polysaccharide from *Castanea mollissima* Blume: preparation, characteristics and antitumor activities in vitro and in vivo, *Carbohydr. Polym.* 240 (2020) 116323.
- [24] G. Du, Y. Liu, J. Zhang, S. Fang, C. Wang, Microwave-assisted extraction of dandelion root polysaccharides: extraction process optimization, purification, structural characterization, and analysis of antioxidant activity, *Int. J. Biol. Macromol.* 299 (2025).
- [25] Q. Su, S. Cai, Q. Duan, W. Huang, Y. Huang, P. Chen, F. Xie, Combined effect of heat moisture and ultrasound treatment on the physicochemical, thermal and structural properties of new variety of purple rice starch, *Int. J. Biol. Macromol.* 261 (2024) 129748.
- [26] X. Wu, Q. Zhang, J. Zhang, B. Zhang, X. Wu, X. Yan, Effect of *Cyperus esculentus* polysaccharide on *Cyperus esculentus* starch: pasting, rheology and in vitro digestibility, *Food Chem. X* 22 (2024) 101511.
- [27] S. Han, Y. Wu, S. Chen, J. Wang, Z. Bai, P. Li, C. Yue, D. Luo, Effects of *Eucommia ulmoides* leaf powder on the gelatinization, rheology, and gel properties of sweet potato starch, *Lwt* 203 (2024) 116428.
- [28] X.-R. Kong, Z.-Y. Zhu, X.-J. Zhang, Y.-M. Zhu, Effects of *Cordyceps* polysaccharides on pasting properties and in vitro starch digestibility of wheat starch, *Food Hydrocoll.* 102 (2020) 105604.
- [29] Y. Ren, L. Jiang, W. Wang, Y. Xiao, S. Liu, Y. Luo, M. Shen, J. Xie, Effects of *Mesona chinensis* Benth polysaccharide on physicochemical and rheological properties of sweet potato starch and its interactions, *Food Hydrocoll.* 99 (2020) 105371.
- [30] M. Zhang, J.B. Golding, P. Pristijono, Y. Yu, P. Wang, G. Chen, Y. Li, J. Si, H. Yang, Effects of Huangjiing polysaccharides on the properties of sweet potato starch, *Lwt* 204 (2024) 116474.
- [31] D. Qiao, Y. Huang, G. Zhao, Y. Zhang, X. Hou, B. Zhang, F. Jiang, Small and large oscillatory shear behaviors of gelatin/starch system regulated by amylose/amylopectin ratio, *Food Hydrocoll.* 142 (2023) 108780.
- [32] Y. Fu, J. Zhou, D. Liu, J.M. Castagnini, F.J. Barba, Y. Yan, X. Liu, X. Wang, Effect of mulberry leaf polysaccharides on the physicochemical, rheological, microstructure properties and in vitro starch digestibility of wheat starch during the freeze-thaw cycles, *Food Hydrocoll.* 144 (2023) 109057.
- [33] X. Yan, D.J. McClements, S. Luo, C. Liu, J. Ye, Recent advances in the impact of gelatinization degree on starch: structure, properties and applications, *Carbohydr. Polym.* 340 (2024) 122273.
- [34] L. Wang, G. Li, L. Zhu, Y. Gao, Y. Wei, Y. Sun, Y. Xu, Preparation and characterization of carboxymethylated *Anemarrhena asphodeloides* polysaccharide and its effect on the gelatinization of wheat starch, *Int. J. Biol. Macromol.* 277 (2024) 134419.
- [35] Z. Wang, Z. Zhong, B. Zheng, Y. Zhang, H. Zeng, Effects of *Porphyra haitanensis* polysaccharides on gelatinization and gelatinization kinetics of starches with different crystal types, *Int. J. Biol. Macromol.* 242 (2023) 125117.
- [36] Y. Zhang, Y. Wang, B. Yang, X. Han, Y. He, T. Wang, X. Sun, J. Zhao, Effects of zucchini polysaccharide on pasting, rheology, structural properties and in vitro digestibility of potato starch, *Int. J. Biol. Macromol.* 253 (2023) 127077.
- [37] J. Wang, Z. Yu, X. Zhang, J. Yang, Y. Luo, M. Wu, Q. Wu, C. Wang, Effect of feruloylated arabinoxylan on the retrogradation and digestibility properties of pea starch during short-term refrigeration: dependence of polysaccharide structure and bound ferulic acid content, *Int. J. Biol. Macromol.* 257 (2024) 128524.
- [38] X. Zhang, Z. Liu, L. Wang, X. Lan, G. He, D. Jia, Effect of hydroxypropyl distarch phosphate on the retrogradation properties of sterilized pea starch jelly and its possible mechanism, *Int. J. Biol. Macromol.* 247 (2023) 125629.
- [39] J. Zheng, N. Wang, J. Yang, Y. You, F. Zhang, J. Kan, L. Wu, New insights into the interaction between bamboo shoot polysaccharides and lotus root starch during gelatinization, retrogradation, and digestion of starch, *Int. J. Biol. Macromol.* 254 (2024) 127877.
- [40] Y. Zhuang, Y. Wang, H. Yang, Effects of cation valence on swelling power, solubility, pasting, gel strength characteristics of potato starch, *Food Chem.* 434 (2024) 137510.
- [41] X. Cui, C. Guan, H. Wang, Q. Liu, L. Zhang, Z. Wang, X. Zhang, *Chlamydomonas reinhardtii* polysaccharides retard rice starch retrogradation by weakening hydrogen bond strength within starch double helices, *Int. J. Biol. Macromol.* 296 (2025) 139570.
- [42] R. Zhou, Y. Wang, Z. Wang, K. Liu, Q. Wang, H. Bao, Effects of *Auricularia auricula-judae* polysaccharide on pasting, gelatinization, rheology, structural properties and in vitro digestibility of kidney bean starch, *Int. J. Biol. Macromol.* 191 (2021) 1105–1113.
- [43] J. Wang, H. Yang, L. Luo, H. Ye, H. Xu, Y. Sun, L. Gong, H. Yang, Persimmon leaf polyphenols as potential ingredients for modulating starch digestibility: effect of starch-polyphenol interaction, *Int. J. Biol. Macromol.* 270 (2024) 132524.
- [44] W. Liu, J. Xu, X. Shuai, Q. Geng, X. Guo, J. Chen, T. Li, C. Liu, T. Dai, The interaction and physicochemical properties of the starch-polyphenol complex: polymeric proanthocyanidins and maize starch with different amylose/amylopectin ratios, *Int. J. Biol. Macromol.* 253 (2023) 126617.
- [45] F. Xie, H. Zhang, Y. Xia, L. Ai, Effects of tamarind seed polysaccharide on gelatinization, rheological, and structural properties of corn starch with different amylose/amylopectin ratios, *Food Hydrocoll.* 105 (2020) 105854.
- [46] M. Yu, B. Liu, F. Zhong, Q. Wan, S. Zhu, D. Huang, Y. Li, Interactions between caffeic acid and corn starch with varying amylose content and their effects on starch digestion, *Food Hydrocoll.* 114 (2021) 106544.
- [47] M. He, X. Wu, T. Gao, L. Chen, F. Teng, Y. Li, Effects of ultrasonic and chemical dual modification treatments on the structural, and properties of cornstarch, *Food Chem.* 451 (2024) 139221.
- [48] J. Zhou, Z. Jia, M. Wang, Q. Wang, F.J. Barba, L. Wan, X. Wang, Y. Fu, Effects of *Laminaria japonica* polysaccharides on gelatinization properties and long-term retrogradation of wheat starch, *Food Hydrocoll.* 133 (2022) 107908.
- [49] Y. Gu, X. Zhang, S. Song, Y. Wang, B. Sun, X. Wang, S. Ma, Structural modification of starch and protein: from the perspective of gelatinization degree of oat flour, *Int. J. Biol. Macromol.* 260 (2024) 129406.
- [50] J. Kuang, J. Huang, W. Ma, C. Min, H. Pu, Y.L. Xiong, Influence of reconstituted gluten fractions on the short-term and long-term retrogradation of wheat starch, *Food Hydrocoll.* 130 (2022) 107716.
- [51] Y. Zhu, C. Dong, F. Chi, X. Gu, L. Liu, L. Yang, Effects of cactus polysaccharide on pasting, rheology, structural properties, in vitro digestibility, and freeze-thaw stability of rice starch, *Foods* 13 (15) (2024) 2420.
- [52] N. Xu, P. Yu, H. Zhang, X. Ji, P. Wu, L. Zhang, X. Wang, Effects of *Laminaria japonica* polysaccharide and coumaric acid on pasting, rheological, retrogradation and structural properties of corn starch, *Int. J. Biol. Macromol.* 263 (2024) 130343.
- [53] S. Cai, Q. Su, Q. Zhou, Q. Duan, W. Huang, W. Huang, X. Xie, P. Chen, F. Xie, Purple rice starch in wheat: effect on retrogradation dependent on addition amount, *Int. J. Biol. Macromol.* 268 (2024) 131788.
- [54] N. Meng, Z. Kang, P. Jiang, Y. Liu, M. Liu, Q. Li, Effects of fucoidan and ferulic acid on potato starch: pasting, rheological and retrogradation properties and their interactions, *Food Hydrocoll.* 150 (2024) 109635.
- [55] Z. Yu, Y.-S. Wang, H.-H. Chen, Q.-Q. Li, Q. Wang, The gelatinization and retrogradation properties of wheat starch with the addition of stearic acid and sodium alginate, *Food Hydrocoll.* 81 (2018) 77–86.
- [56] J. Rumpf, R. Burger, M. Schulze, Statistical evaluation of DPPH, ABTS, FRAP, and Folin-Ciocalteu assays to assess the antioxidant capacity of lignins, *Int. J. Biol. Macromol.* 233 (2023) 123470.
- [57] O.P.N. Yarley, A.B. Kojo, C. Zhou, X. Yu, A. Gideon, H.H. Kwadwo, O. Richard, Reviews on mechanisms of in vitro antioxidant, antibacterial and anticancer activities of water-soluble plant polysaccharides, *Int. J. Biol. Macromol.* 183 (2021) 2262–2271.
- [58] P.A.R. Fernandes, M.A. Coimbra, The antioxidant activity of polysaccharides: a structure-function relationship overview, *Carbohydr. Polym.* 314 (2023) 120965.
- [59] J. Gao, L. Zhu, J. Huang, L. Li, Y. Yang, Y. Xu, Y. Wang, L. Wang, Effect of dandelion root polysaccharide on the pasting, gelatinization, rheology, structural properties and in vitro digestibility of corn starch, *Food Funct.* 12 (15) (2021) 7029–7039.